

# DEVELOPMENT OF CASCADE FULL- BRIDGE INVERTER WITH VARIOUS PWM TECHNIQUES

M.Kaleeswari, S.Vijayabaskar

**Abstract**— Cascade H-bridge inverter has been widely used in various applications, especially where separate DC sources naturally exist in the places, such as photovoltaics, fuel cells, battery energy storage, and electric vehicle drives. The advantages of cascade type inverters include the capability of reaching higher output voltage level by using standard lower voltage devices, and the modular design concept which makes the maintenance less burdensome. Thus, the cascade H-bridge inverter is based on a series connection of several single H-bridge inverters where two active devices are in one leg, it still faces shoot-through problems and it needs soft switching technique. The proposed cascade dual buck full-bridge inverter eliminates the possibility of shoot-through problems which is the major failure of traditional voltage source inverters. Thereby, it does not need dead time which fully utilizes the pulse width modulated voltage and transfers total desired energy to the output. It can use high-voltage power MOSFETs without the complexity of soft-switching assisting circuits to improve the system efficiency. Hybrid PWM technique leads to better performance of the cascade dual-buck full-bridge inverter as compared to cascade H bridge, it provides less output current ripple and harmonics, no zero-crossing distortion, and higher efficiency. The proposed method is implemented using MATLAB/SIMULINK version 2008b.

**Index Terms**— Pulse width modulation, Zero voltage switching, Zero current switching, unipolar switching scheme, Carrier voltage, Reference voltage.

## I. INTRODUCTION

In the past two decades, renewable energy has gained tremendous attention thanks to its environmentally-friendly feature as well as its ability to offer more cost-effective options to meet the demand of electricity market. Distributed generation (DG) based on renewable energy provides power in the vicinity of loads, which reduces the loss through power transmission and improves the power quality to the loads. In addition, the DG can be utilized in a remote village or rural area where the grid

is not available. It can also be used as a backup source when the grid is gone. Solar power, wind power, and fuel cells are widely used for distributed generation. Because the first two energy sources do not need extra fuel, the installation of photovoltaic modules (PV) and wind turbines increased at a rate of 20-40% per year in the last few years. Though fuel cells have a higher fuel cost compared to solar and wind power, they are considered better for the system stability because they are not susceptible to the weather for power generation. Grid-tie control of renewable energy and DG systems, such as fuel cell, photovoltaics, and wind power, are important research topics nowadays. Various circuit topologies and control methods have been proposed to improve the efficiency and to enhance the performance and reliability.

With its flexible modular design, transformerless connection, extended output voltage and output power, low maintenance and high fault tolerance, the cascade inverters are good candidates for low-cost utility new type of cascade inverter utilizing the dual-buck type inverter cells to stack the multilevel ac output voltage is proposed for a highly reliable, high-efficiency, and potentially low cost inverter that can be used in different renewable energy and distributed generation applications. Among various multilevel voltage-source inverters, the most commonly used and commercially available ones are the neutral-point-clamped inverter, flying capacitor inverter and cascade H-bridge inverter [1]-[5]. Cascade inverters are with separate DC sources, and each DC source is associated with a single-phase inverter while the ac terminals of each inverter are connected in series [6]-[9]. It was first invented by Richard H. Baker back in 1975. The cascade types of inverters are capable of reaching higher output voltage level by using commercially standard lower voltage devices and components, and it features the modular design concept which makes the maintenance less burdensome [10]-[12]. In medium voltage AC drives application, Robicon Corporation promoted cascade H-bridge inverters and claimed numerous advantages of their products, including low voltage and current THD level and optional degrees of redundancy with electronic bypass [13]-[15]. The cascade inverters are well suited for utility interface of various renewable energy sources, such as photovoltaics, fuel cells, led to cost effective sophisticated control strategies with easy calculation and implementation

M.Kaleeswari, M.E (PED) II year, P.A college of Engineering and Technology, Tamilnadu, India.  
Dr.S.Vijayabaskar, Associate professor, Department of EEE, P.A college of Engineering and Technology, Pollachi, Tamilnadu, India.

## II. PHASE SHIFT CONTROL

One of the significant characteristics of single-unit dual-buck type inverter is that the switch is selectively working based on the direction of output current. From the operation modes of single-unit half-bridge dual-buck inverter, it can clearly see that when  $i_1$  is positive,  $S_{1p}$  and  $D_{1p}$  are the working pair, and when  $i_1$  is negative,  $S_{1n}$  and  $D_{1n}$  are the working pair. This distinctive operation leads to its inherent drawback, current zero-crossing distortion, which will be explained in detail below. This issue can be passively mitigated by turning on both  $S_{1p}$  and  $S_{1n}$  near zero-crossing period. This remedy is against the operating principle and the best feature of dual-buck type inverter, high reliability by avoiding turning on both active switches at the same time. In addition, this passive measure results in higher switching losses because at zero-crossing period two switches are switching while the original goal of dual-buck inverter is only one switch operates at any given time. Thanks to cascade topology, it opens the door to actively solving this current zero crossing distortion by using phase-shift control scheme. With phase-shifted PWM fed to different cascade units, it theoretically reduce the current zero-crossing distortion. In addition, the phase-shift control greatly increases the equivalent switching frequency by  $N$  times than that of single-unit inverter, which leads to significantly lower current ripple or smaller passive filter component selections.

## III. PHOTOVOLTAIC GENERATOR

A Photovoltaic generator consists of an array of solar panels, normally series and parallel connected cells to obtain desired voltage and current. Any photovoltaic generator can be represented by a current source shunted with a parallel combination of diode and resistor ( $R_{sh}$ ), which represents the leakage current and series resistor represented by leakage resistance ( $R_{se}$ ). Each solar cell produces electricity in DC form from solar energy. Figure 3.1 shows the representation of solar panel generator.

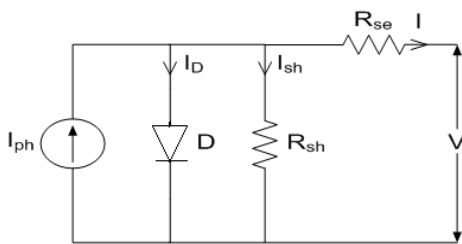


Figure 3.1 Photovoltaic Cell Model

### A. Design

The volt-ampere equation of the photovoltaic system is given

$$I = I_{ph} - I_0 \left( e^{\frac{V+IR_s}{av_t}} - 1 \right) - \frac{V+IR_s}{R_{sh}} \quad (3.1)$$

$$V_t = \frac{N_s K T_c}{q} \quad (3.2)$$

### B. Temperature and irradiation correction factors

The change in output voltage and output current with temperature change can be designated by temperature coefficients  $C_{TV}$  &  $C_{TI}$ .

$$C_{TV} = 1 + \beta_T (T_a - T_x) \quad (3.3)$$

$$C_{TI} = 1 + \frac{\gamma_T}{S_c} (T_a - T_x) \quad (3.4)$$

$$\beta_T = 0.004, \gamma_T = 0.06$$

Change in the cell irradiation level causes changes in photocurrent and cell temperature which causes a change in cell voltage. The change in output voltage and photocurrent with change in irradiation can be represented by  $C_{SV}$  &  $C_{SI}$  and the change in temperature be  $\Delta T_c$

$$C_{SV} = 1 + \beta_T \alpha_S (S_x - S_c) \quad (3.5)$$

$$C_{SI} = \frac{1}{S_c} (S_x - S_c) \quad (3.6)$$

$$\Delta T_c = \alpha_S (S_x - S_c) \quad (3.7)$$

The new values of cell voltage and photocurrent by considering the changes in temperature and solar irradiation can be found by the following equation.

$$V_{CX} = C_{SV} C_{TV} V \quad (3.8)$$

The operating principle and analysis of cascade dual buck converter and PV system has been explained in the above chapter. New series of cascade dual-buck inverters has been proposed based on single-unit dual-buck inverters. The cascade dual-buck inverter has all the merits of traditional cascade inverters, and improves on its reliability by eliminating shoot-through worries and dead-time concerns. With the adoption of phase-shift control, the cascade dual-buck inverter solves the inherent current zero-crossing distortion problem of single-unit dual-buck inverter. One of the significant characteristics of single-unit dual-buck type inverter is that the switch is selectively working based on the direction of output current.

## IV. CASCADE DUAL-BUCK FULL-BRIDGE INVERTER

The dual-buck full-bridge inverter does not need dead time, and totally eliminates the shoot-through concerns, which leads to greatly enhanced system reliability. The body diode of MOSFET never conducts, and the external diodes  $D_1$  to  $D_4$  can be independently selected to minimize switching losses. The traditional bipolar sinusoidal PWM (SPWM) used

on dual-buck full-bridge inverter results in zero-crossing distortion of the output voltage and current, which will be explained in next section. Even though the topology adopts MOSFET, the dual-buck full-bridge inverter is still the hard-switching VSI. To further reduce the switching loss in power devices and passive filter components, and at the same time alleviate the zero-crossing distortion problem, an asymmetrical half-cycle unipolar (AHCU) PWM technique for dual-buck full-bridge inverter is proposed. This AHCU PWM cuts down the switching loss of power MOSFETs to half by maintaining one active switch without switching during half-cycle of inverter output current. It also reduces the output current ripple, and therefore leads to less power loss in passive components of the inverter. It compensates for the zero-crossing distortion problem found in ordinary PWM operated dual-buck inverters, and practically eliminates this drawback. The next section analyzes the traditional bipolar SPWM technique and points out its disadvantages when applied to dual-buck full-bridge inverters. Then the AHCU PWM method is proposed and elaborated on to solve the zero-crossing distortion problem and improve the system efficiency.

Figure 4.1 shows the proposed topology of the cascade dual-buck full-bridge inverter. It consists of  $N$  units of single dual-buck full-bridge inverter. Each unit is composed of four power MOSFETs and four fast recovery diodes. Each unit has two output ports,  $i_p$  and  $i_N$  ( $i=1, 2, \dots, N$ ). To realize the cascade topology, connect the  $i_N$  port of the  $i_{th}$  unit with the  $(i+1)_p$  port of the  $(i+1)_{th}$  unit, and use port  $1_p$  and  $N_N$  as the final output ports. The bipolar PWM, unipolar PWM, and phase-shifted PWM for cascade dual-buck full-bridge inverter is presented in this chapter. It has been found out that the PWM combination technique, which means the use of two PWM methods at the same time, can lead to elimination of zero-crossing distortion, reduced current ripple, and increased system efficiency.

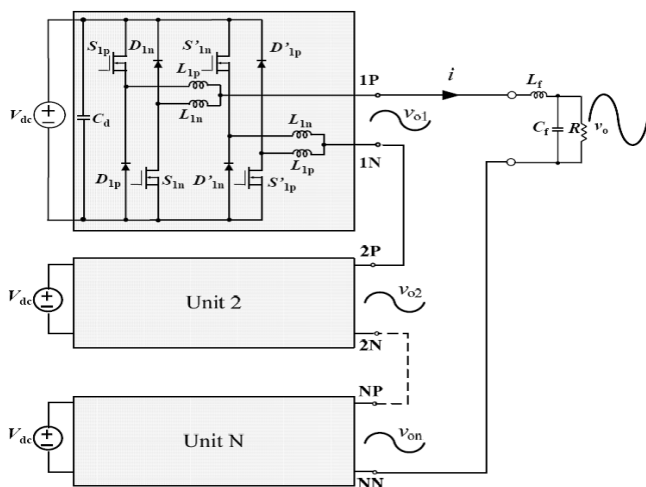
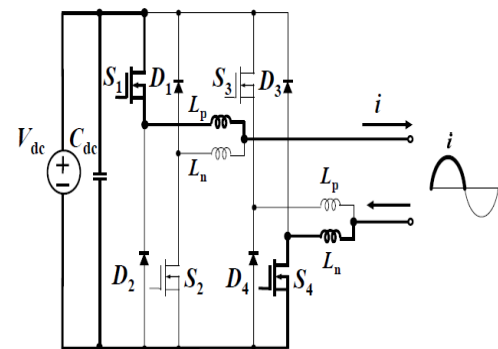


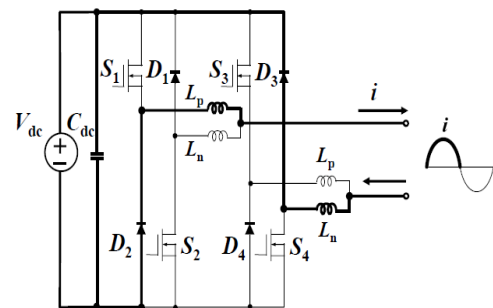
Figure 4.1 Topology of cascade dual-buck full-bridge inverter

## V. TRADITIONAL BIPOLAR SPWM

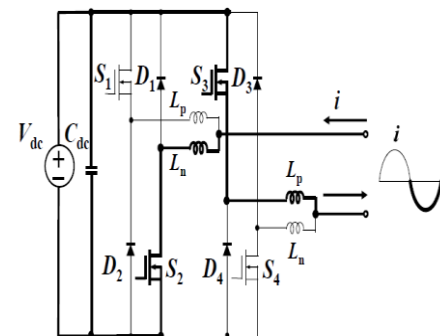
One of the significant features of a dual-buck full-bridge inverter is that the switch is selectively working based on the direction of output current. Figure 5.1 shows the operation modes of dual-buck full-bridge inverter under traditional bipolar SPWM. When the output current  $i$  is in the positive half cycle,  $(S_1, D_2)$  and  $(S_4, D_3)$  are the two pairs of working devices. The energy is pumped out when  $S_1$  and  $S_4$  are turned on, shown in Figure 5.1(a).  $D_2$  and  $D_3$  are freewheeling when  $S_1$  and  $S_4$  are turned off, shown in Figure 5.1 (b). Likewise, when the output current  $i$  is negative, the operation shifts to  $(S_2, D_1)$  and  $(S_3, D_4)$ . The DC side energy is transferred to ac side by turning on  $S_2$  and  $S_3$ , indicated in Figure 5.1 (c).  $D_1$  and  $D_4$  start to conduct the current when  $S_2$  and  $S_3$  are off, shown in Figure 5.1 (d).



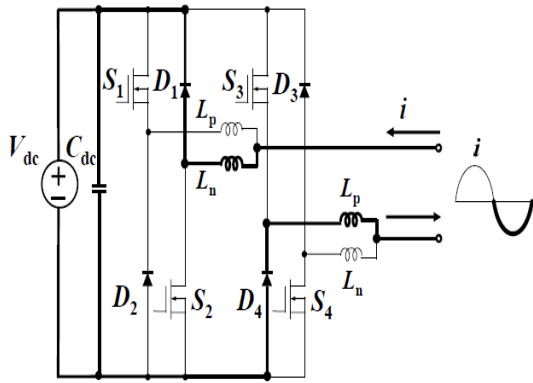
(a) Positive current,  $S_1$  and  $S_4$  turned on



(b) Positive current,  $D_2$  and  $D_3$  free-wheeling



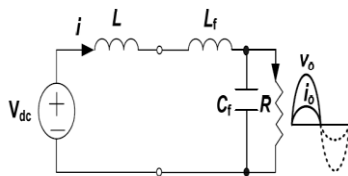
(c) Negative current,  $S_2$  and  $S_3$  turned on



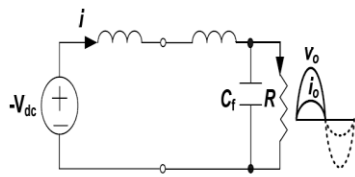
(d) Negative current,  $D_1$  and  $D_4$  free-wheeling

Figure 5.1 Operation modes under traditional bipolar SPWM

Figure 5.2 shows the equivalent circuit of the dual-buck full-bridge inverter at the output current positive half cycle, which relates to the operation mode in Figure 5.2 (a) and (b).  $L_f$  and  $C_f$  are the filter inductor and capacitor.  $L$  is the output inductor, and is equal to the sum of  $L_p$  and  $L_n$ . Figure 5.2 shows the gate signal of  $S_1$  and  $S_4$ , and the current through output inductor  $i$ . The shaded area of Figure 4.4 corresponds to the operation mode shown in Figure 5.2 (a).  $D_s$  is the duty cycle for the switch  $S_1$  and  $S_4$ , and under traditional bipolar SPWM,  $0.5 \leq D_s \leq 1$ .



(a)  $S_1$  and  $S_4$  on



(b)  $D_2$  and  $D_3$  free-wheeling

Figure 5.2 Equivalent circuit of dual-buck full-bridge inverter when output current is positive

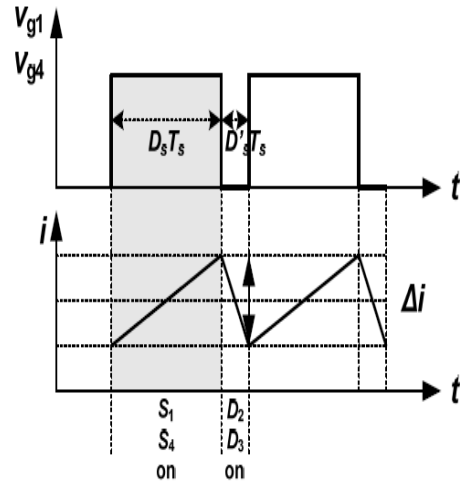


Figure 5.3 Gate signal of  $S_1$  and  $S_3$  with current  $i$  through output inductor

The current ripple of  $i$  can be derived from Figure 5.2 and Figure 5.3 as follows

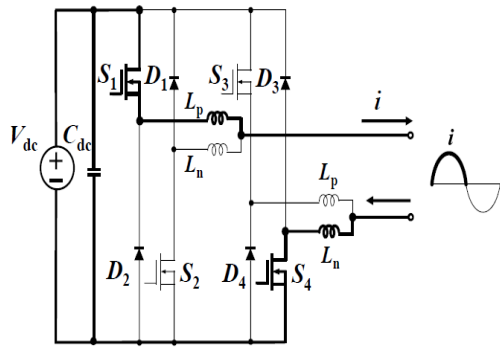
$$\Delta i = \frac{(V_{dc} - V_o) D_s T_s}{L + L_f} \quad (5.1)$$

It can be seen that at the zero-crossing period,  $D_s$  is approaching 0.5. Therefore, the current ripple at zero-crossing region is not zero.

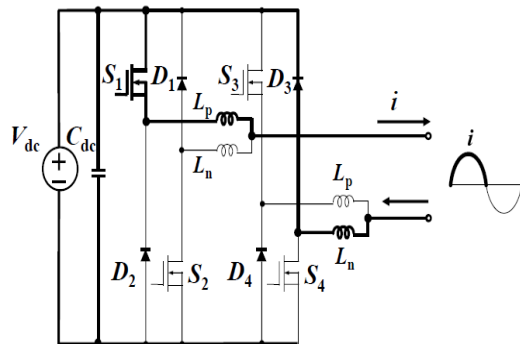
It is also known that with traditional bipolar SPWM, all the active switches operate at high switching frequency. For example, at the positive half cycle,  $S_1$  and  $S_4$  are turned on and off at the same time within every switching period. This leads to higher switching losses. In addition, under this PWM scheme, the current ripple is higher, which results in higher losses in filter components as well.

#### VI. ASYMMETRICAL HALF-CYCLE UNIPOLAR (AHCU) PWM SCHEME

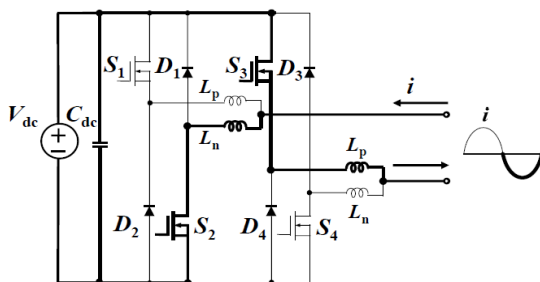
To address the issues of zero-crossing distortion and higher switching losses caused by traditional bipolar PWM, an asymmetrical half-cycle unipolar (AHCU) PWM scheme is proposed for dual-buck full-bridge inverter. Figure 6.1 shows the operation modes of dual-buck full-bridge inverter under this new PWM. When the output current is at the positive half cycle,  $S_1$  is always turned on, shown in Figure 6.1 (a) and (b).  $S_4$  is the switching device for this positive half cycle. When  $S_4$  is on, the output voltage is  $V_{DC}$ , and when it is off,  $D_3$  freewheels with output voltage equal to zero. Likewise, when the output current is at the negative half cycle,  $S_2$  is kept on, with  $S_3$  and  $D_4$  working at the switching frequency, shown in Figure 6.1 (c) and (d). The output PWM voltage is  $-V_{DC}$  and zero.



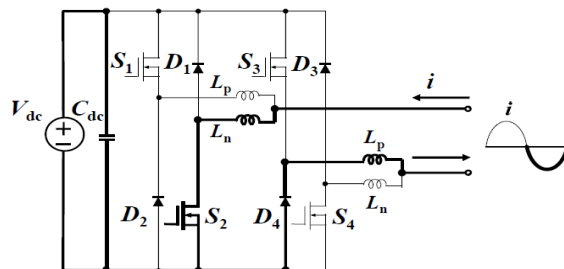
(a) Positive current,  $S_1$  and  $S_4$  turned on



(b) Positive current,  $S_1$  on and  $D_3$  free-wheeling



(c) Negative current,  $S_2$  and  $S_3$  turned on

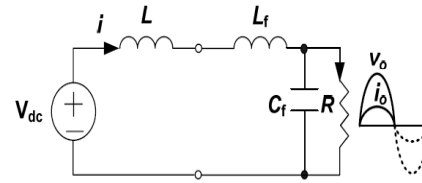


(d) Negative current,  $S_2$  on and  $D_4$  free-wheeling

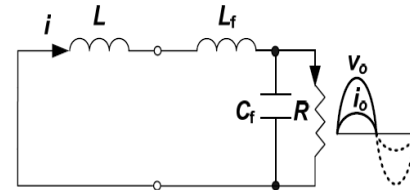
Figure 6.1 Operation modes under AHCU SPWM

Figure 6.1 shows the equivalent circuit under this PWM at the output current positive half cycle, which relates to the operation mode in Figure 6.2 (a) and (b) shows the gate signal of  $S_1$  and  $S_4$ , and the current through output inductor  $i$ . The shaded area of Figure 6.1 corresponds to the operation mode

shown in Figure 6.2 (a).  $D_{sH}$  is the duty cycle for the switch  $S_4$ , and under this AHCU PWM,  $0 \leq D_{sH} \leq 1$ .



(a)  $S_1$  and  $S_4$  on



(b)  $S_1$  on and  $D_3$  freewheeling

Figure 6.2 Equivalent circuit under AHCU PWM when output current is positive

The current ripple of  $i$  can be derived from Figure 6.1 and Figure 6.2

$$\Delta i = \frac{(V_{dc} - V_o)D_{sH}T_s}{L + L_f} \quad (6.1)$$

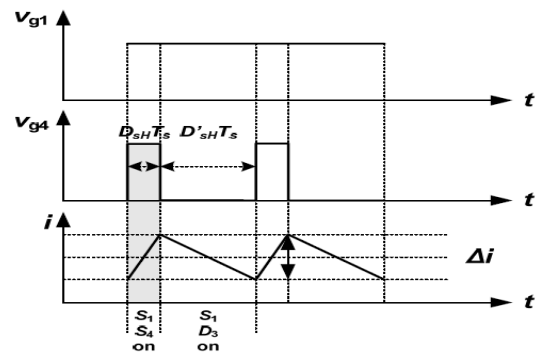


Figure 6.3 Gate signal of  $S_1$  and  $S_4$  with current  $i$  through output inductor

Compared to the current ripple equation for traditional bipolar SPWM, it is clear that at zero-crossing period, the current ripple under this PWM is close to zero because  $D_{sH}$  is close to zero even though  $V_{DC}$  is high. Theoretically, when the positive half cycle current connects with the negative half-cycle current, there is no current jump at all at zero-crossing region. From Figure 6.1 and Figure 6.3, we can see that under this AHCU PWM scheme; only one active switch operates at switching frequency at any instant. Compared to the traditional bipolar SPWM where two active switches run at switching frequency, the switching loss of the devices is theoretically cut down by half.

VII. SIMULATION DIAGRAM AND RESULT

The analysis, design and implementation of the cascade dual-buck inverters has been carried out and presented in this chapter. Compared to traditional cascade inverters, cascade dual-buck inverters have enhanced system reliability, no dead time and shoot-through concerns and they can achieve lower switching losses with the help of using power MOSFETs.

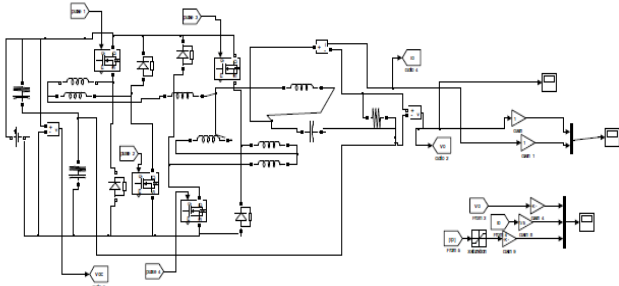


Figure 7.1 Simulation diagram of Single dual-buck inverter

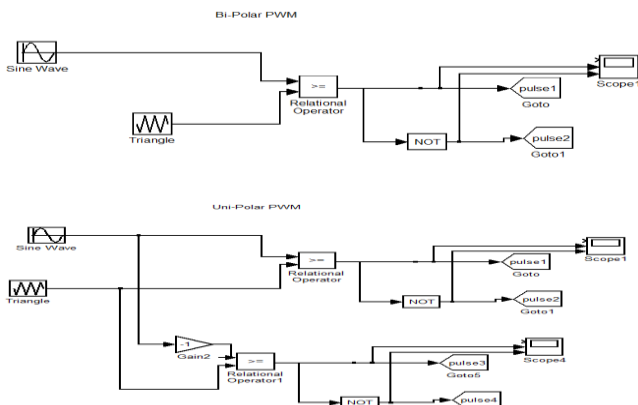
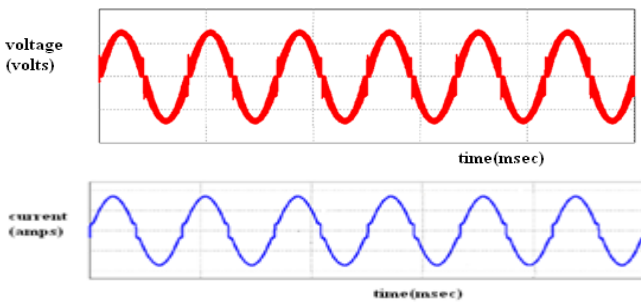
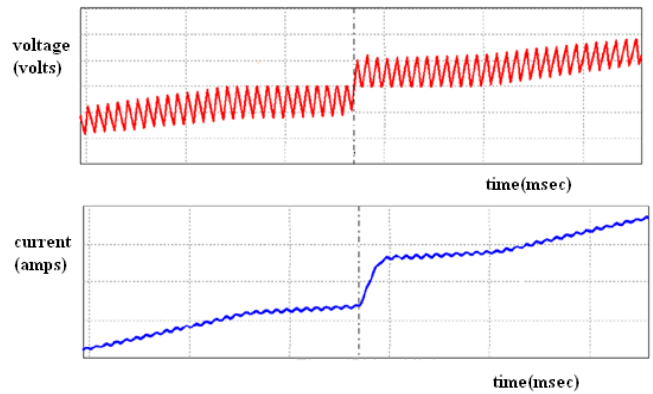


Figure 7.2 Simulation diagram of Bipolar PWM and uni-polar PWM

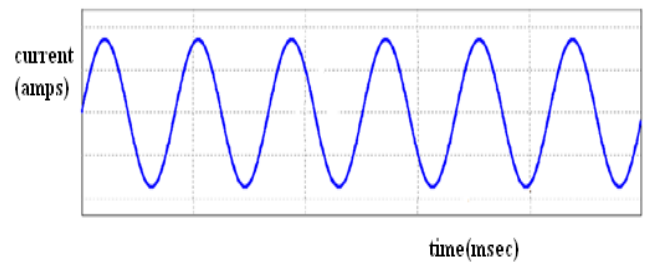
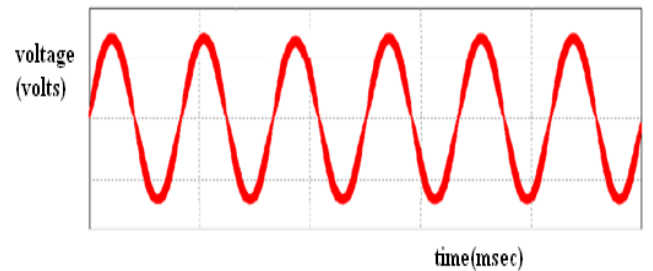
The output of sliding mode controller is the actual speed which is estimated from motor current and voltage as its input. The controller is designed with the help of above equations which is described in section VI.



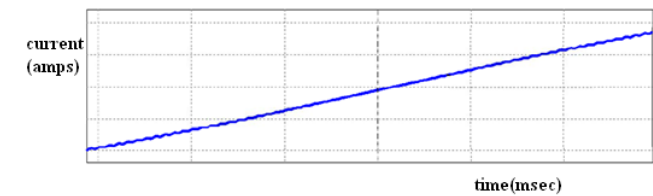
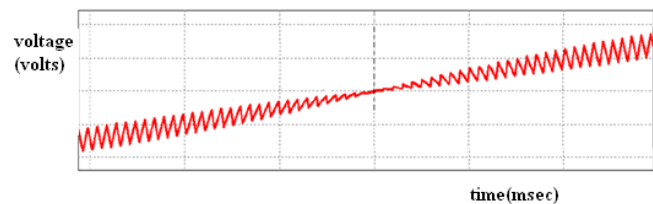
(a) Waveform of Output Voltage and current



(b) Waveforms of voltage and current at zero crossing  
 Figure 7.2 Simulation result of dual-buck full-bridge inverter under traditional bipolar PWM



(a) Waveforms of voltage and current



(b) Waveforms of voltage and current at zero crossing

Figure 7.3 Simulation result of dual-buck full-bridge inverter under AHCU PWM

## VIII. CONCLUSION

The analysis, design and implementation of the cascade dual-buck inverters has been carried out and presented in this thesis. Compared to traditional cascade inverters, cascade dual-buck inverters have enhanced system reliability, no dead time and shoot-through concerns and they can achieve lower switching losses with the help of using power MOSFETs.

Evaluation of different PWM schemes is performed on cascade dual-buck full-bridge inverters. Several PWM techniques are analyzed and compared, including bipolar PWM, unipolar PWM and phase-shifted PWM. It has been found out that a PWM combination technique with the use of two out of the three PWMs leads to better performance in terms of less output current ripple and harmonics, no zero crossing distortion, and higher efficiency. Simulation results are presented to validate the system.

## REFERENCES

- [1] Arash A. Boora, Alireza Nami, Firuz Zare, Arindam Ghosh, and Frede Blaabjerg, ( Oct 2010 ) “Voltage-Sharing Converter to Supply Single Phase Asymmetrical Four-Level Diode Clamped Inverter With High Power Factor Loads”, IEEE Trans On Power Electronics, Vol. 25, No. 10, Pp. 2507-2520.
- [2] Baoming Ge, Fang Zheng Peng, Anibal T. de Almeida, and Haitham Abu-Rub, ( Aug 2010 ) “An Effective Control Technique for Medium Voltage High-Power Induction Motor Fed by Cascaded Neutral-Point-Clamped Inverter”, IEEE Trans On Industrial Electronics, Vol. 57, No. 8, pp. 2659-2668.
- [3] C. Attaianese, M. Di Monaco, and G. Tomasso, (2010) “Three-Phase Three-Level Active NPC Converters for High Power System”, International Symposium on Power Electronics, Electrical Drives, Automation and Motion, pp. 204-209, Speedam.
- [4] Grain P. Adam, Stephen J. Finney, Ahmed M. Massoud, and Barry W. Williams, ( Aug 2008 ) “Capacitor Balance Issues of the Diode-Clamped Multilevel Inverter Operated in a Quasi Two State Mode” IEEE Trans On Industrial Electronics, Vol. 55, NO. 8, pp. 3088- 3099 .
- [5] H. K. Al-Hadidi, A. M. Gole, and David A. Jacobson, (April 2008) “A Novel Configuration for a Cascade Inverter-Based Dynamic Voltage Restorer With Reduced Energy Storage Requirements”, IEEE Trans. On Power Delivery, Vol. 23, No. 2, pp. 881-888.
- [6] J. Liu, and Y. Yan, (2003) “A Novel Hysteresis Current Controlled Dual Buck Half Bridge Inverter”, in *Proc. IEEE PESC*, 2003, pp. 1615-1620.
- [7] Jeffrey Ewanchuk, John Salmon, and Behzad Vafakhah, (Sept/Oct 2011) “A Five-/Nine-Level Twelve Switch Neutral-Point-Clamped Inverter for High-Speed Electric Drives”, IEEE Trans on Industry Applications, Vol. 47, No. 5, pp. 2145-2153.
- [8] Jin Li, Jinjun Liu, Dushan Boroyevich, Paolo Mattavelli, and Yaosuo Xue, (Dec 2011) “Three-level Active Neutral-Point-Clamped Zero-Current Transition Converter for Sustainable Energy Systems”, IEEE Trans. On Power Electronics, Vol. 26, No. 12, pp. 3680-3693.
- [9] Jin Li, Jinjun Liu, Dushan Boroyevich, Paolo Mattavelli, and Yaosuo Xue, (May 30-June 3, 2011) “Comparative Analysis of Three-Level Diode Neutral-Point-Clamped and Active Neutral-Point-Clamped Zero-Current-Transition Inverters”, 8th International Conference on Power Electronics, pp. 2290-2295.
- [10] Jun Li, Subhashish Bhattacharya, and Alex Q. Huang, (March 2011) “A New Nine-Level Active NPC (ANPC) Converter for Grid Connection of Large Wind Turbines for Distributed Generation”, IEEE Trans On Power Electronics, Vol. 26, No. 3, pp. 961-972.
- [11] Marcelo C. Cavalcanti, Alexandre M. Farias, Kleber C. Oliveira, Francisco A. S. Neves, and João L. Afonso, (Jan 2012) “Eliminating Leakage Currents in Neutral Point Clamped Inverters for Photovoltaic Systems”, IEEE Trans. On Industrial Electronics, Vol. 59, No. 1, pp. 435- 443.
- [12] Pablo Lezana, José Rodríguez, and Diego A. Oyarzún, (March 2008) “Cascaded Multilevel Inverter With Regeneration Capability and Reduced Number of Switches”, IEEE Trans. On Industrial Electronics, Vol. 55, No. 3, pp. 1059-1066.
- [13] Robert Stala, (Sept 2011) “Application of Balancing Circuit for DC-Link Voltages Balance in a Single-Phase Diode-Clamped Inverter With Two Three-Level Legs”, IEEE Trans On Industrial Electronics, Vol. 58, No. 9, pp. 4185-4195.
- [14] Z. Yao, L. Xiao, and Y. Yan, (Aug 2009) “Dual-Buck Full-Bridge Inverter With Hysteresis Current Control”, IEEE Trans. Ind. Electron., vol. 56, no. 8, pp. 3153–3160.
- [15] Zhiguo Pan, Fang Zheng Peng, Keith A. Corzine, Victor R. Stefanovic, John M. (Mickey) Leuthen, and Slobodan Gataric, (Nov/Dec 2005) “Voltage Balancing Control of Diode Clamped Multilevel Rectifier/Inverter Systems” IEEE Trans On Industry Applications, Vol. 41, No. 6, pp. 1698-1706.